Xjenza Online - Journal of Malta Chamber of Scientists
http://www.mcs.org.mt/
Doi: http://dx.medra.org/10.7423/XJENZA.2013.2.08

Research Article

Optical Glauber Modeling in High-Energy Nuclear Collisions

Jurgen Mifsud[1] **and Thorsten Kollegger**[2]
[1]Department of Physics, University of Malta, Malta
[2]CERN, CH-1211, Genéve 23, Switzerland

Abstract. The Optical Glauber Model is used in this study in order to understand the initial conditions in heavy-ion collisions and at the end understand the relationship between the particles produced after the collision. In the first part of this study, the initial geometrical features of the collision as a function of the impact parameter, such as the number of participating nucleons and the number of collisions between nucleons are obtained. Then, after obtaining numerical values for the number of participating nucleons, the study was focused on two distinct particles being produced after the collision and the relationship between them is also determined from the correlation as a function of the impact parameter.

Keywords Optical Glauber model - Impact parameter - Number of participants - Number of nucleon-nucleon collisions - Wood-Saxon.

1 Introduction

In an ultrarelativistic collision of nuclei, the complexity of the collision event is much higher compared with proton-proton collisions, and it seems to be difficult to study how each event occurred. Given the Glauber model, one can trace back each collision and even get some results of the impact parameter, the number of participating nucleons, and also the number of binary nucleon-nucleon collisions.

Section 2 discusses the basic history of the Glauber model, together with the inputs required in order to carry out a Glauber calculation in a high-energy collision. Section 3 discusses the Optical Glauber model in detail, in which all required formulae are derived, and the respective results are also discussed. Section 4 discusses in one way how the Glauber model is related to experimental data, in which the production of particles after a collision is studied. The relationship between these produced particles is also discussed. Finally in section 5, the current status and future applications of the Glauber model are discussed, with a reference to some results obtained during this study.

Correspondence to: J. Mifsud (jurgen.mifsud.10@um.edu.mt)

2 Theoretical Foundations of Glauber Modeling

2.1 A Brief History of the Glauber Model

The Glauber model was developed to resolve the problem of high-energy scattering with composite particles. This idea was of great interest in the fields of both nuclear and particle physics. In 1958, Glauber presented his first collection of various papers and unpublished work from the 1950's. Glauber's work put the quantum theory of collisions of composite objects on a firm basis and provided a consistent description of experimental data for protons colliding with deuterons and larger nuclei. Most striking were the observed dips in elastic peaks, whose position and magnitude were predicted by Glauber's theory, by Czyz and Lesniak in 1967 (Miller et al. 2007).

Bialas et al.'s approach introduced the functions used in this study. For example, they introduced the thickness function and a prototype of the nuclear overlap function. They also introduced the optical limit for analytical and numerical calculations (Miller et al. 2007).

As computational processing increased over the past years, the Glauber Monte Carlo approach has been implemented. This approach was first applied to high-energy heavy ion collisions in the HIJET model (Miller

et al. 2007) and has found its way in practically all A+A simulation codes. This includes HIJING, VENUS and RQMD (Miller et al. 2007).

2.2 Inputs to Glauber Calculations

2.2.1 Nuclear charge densities

The nucleon density is usually parameterized by a Fermi distribution with three parameters, commonly known as the Wood-Saxon nucleon density;

$$\rho(r) = \rho_0 \frac{1 + w(r/R)^2}{1 + exp\left(\frac{r-R}{a}\right)} \tag{1}$$

where ρ_0 corresponds to the nucleon density in the center of the nucleus, R corresponds to the nuclear radius, a to the skin depth, and w characterizes deviations from a spherical shape. This is the model that is going to be used in the calculations that follow, although a reference to the hard sphere model is also made where necessary. The hard sphere model treats the density distribution as a step function, in which the density is constant within the nuclear radius and then it goes down to zero everywhere outside the nuclear radius range. It is represented by the following equation,

$$\rho(r) = \begin{cases} \rho_0 & , r < R \\ 0 & , r \geq R \end{cases} \tag{2}$$

In this analysis, only Lead(Pb) nuclei are considered. Values of the parameters for Pb-207 are given in Table 1 (Alver et al. 2008).

R [fm]	6.62
a [fm]	0.546
w [fm]	0

Table 1: List of values of the parameters for Pb-207 nuclei.

Using the values defined in Table 1, the density distribution of Pb-207 is plotted (Fig.(1)), where the solid line is representing the density distribution given by the Wood-Saxon nucleon density, and the dashed line represents the distribution given by the hard sphere model.

2.2.2 Inelastic nucleon-nucleon cross section

The Glauber model assumes that the nucleons collide inelastically and the number of charged particles produced on each collision to remain the same on an average. As the cross section involves processes with low momentum transfer, it is impossible to calculate this using perturbative quantum chromodynamics. Thus, the measured inelastic nucleon-nucleon cross section (σ^{NN}) is used as an input and provides the only nontrivial beam-energy

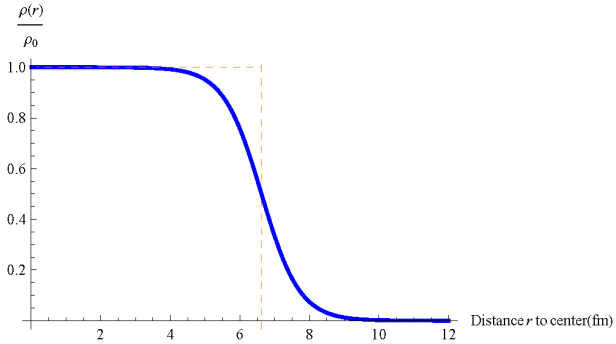

Figure 1: Density distribution for Pb-207 nuclei.

dependence for Glauber calculations. Diffractive and elastic processes are not considered in this analysis, although they are measured experimentally and studied for other research interests (Miller et al. 2007; Esha 2012).

3 Optical Glauber Model

In the following formalism of the Optical Glauber model, it is assumed that at sufficiently high energies, the nucleons will carry sufficient momentum that they will be undeflected as the nuclei pass through each other and also that the nucleons move independently in the nucleus and that the size of the nucleus is large compared to the nucleon-nucleon force.

3.1 Deriving expressions

The base of the analytical formulae is illustrated diagramatically (Fig.(2)), in which two heavy ions, target A and projectile B, are shown colliding at relativistic speeds with impact parameter $\overrightarrow{b}$ (Miller et al. 2007). In order to derive the equations that follow, one shall consider two flux tubes located at a displacement $\overrightarrow{s}$ with respect to the center of the target nucleus and hence a displacement of $\overrightarrow{s} - \overrightarrow{b}$ from the center of the projectile. During the collision these tubes overlap, and this is what one is interested in, in order to determine the particles being produced during the collision.

The probability per unit transverse area of a given nucleon being located in the target flux tube is given by,

$$\hat{T}_A(\overrightarrow{s}) = \int \hat{\rho}_A(\overrightarrow{s}, z_A) dz_A \tag{3}$$

where $\hat{\rho}_A(\overrightarrow{s}, z_A)$ is the probability per unit volume, normalized to unity, for finding the nucleon at location $(\overrightarrow{s}, z_A)$. Similarly, the equation for the projectile nucleon is simply,

$$\hat{T}_B(\overrightarrow{s}) = \int \hat{\rho}_B(\overrightarrow{s}, z_B) dz_B \tag{4}$$

where $\hat{\rho}_B(\overrightarrow{s}, z_B)$ has a similar meaning to the previous one. The information for both $\hat{\rho}_A(\overrightarrow{s}, z_A)$ and $\hat{\rho}_B(\overrightarrow{s}, z_B)$ is obtained through the nuclear density profile of the respective colliding nuclei. Thus, the product

$$\hat{T}_A(\overrightarrow{s})\hat{T}_B(\overrightarrow{s} - \overrightarrow{b})d^2s \tag{5}$$

then gives the joint probability per unit area of nucleons being located in the respective overlapping target and projectile flux tubes of differential area d^2s. One shall define the thickness function $\hat{T}_{AB}(\overrightarrow{b})$, as the integral over the joint probability given by (5), i.e.

$$\hat{T}_{AB}(\overrightarrow{b}) = \int \hat{T}_A(\overrightarrow{s})\hat{T}_B(\overrightarrow{s} - \overrightarrow{b})d^2s \tag{6}$$

One can interpret the thickness function as the effective overlap area for which a specific nucleon in A can interact with a given nucleon in B, indeed it is purely a geometrical factor. The probability of an interaction occurring is then given by

$$\hat{T}_{AB}\sigma_{inel}^{NN} \tag{7}$$

where σ_{inel}^{NN} is the inelastic nucleon-nucleon cross section. Elastic processes lead to very little energy loss and are consequently neglected in the calculation. Once the probability of a given nucleon-nucleon interaction has been found, the probability of having n such interactions between nuclei A and B is given by a binomial distribution,

$$P(n, \overrightarrow{b}) = \begin{pmatrix} AB \\ n \end{pmatrix} [\hat{T}_{AB}(\overrightarrow{b})\sigma_{inel}^{NN}]^n [1 - \hat{T}_{AB}(\overrightarrow{b})\sigma_{AB}^{NN}]^{AB-n} \tag{8}$$

where the first term is the number of combinations for finding n collisions out of AB possible nucleon-nucleon interactions, the second term is the probability for having exactly n collisions, and the last term the probability of exactly $AB - n$ misses.

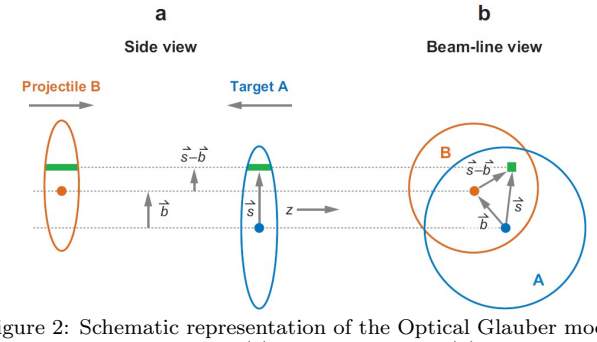

Figure 2: Schematic representation of the Optical Glauber model geometry, with transverse (a) and longitudinal (b) views.

Then the total probability of an interaction between A and B is given by

$$\begin{aligned} \frac{d^2\sigma_{inel}^{AB}}{db^2} &\equiv p_{inel}^{AB}(b) = \textstyle\sum_{n=1}^{AB} P(n, \overrightarrow{b}) \\ &= 1 - [1 - \hat{T}_{AB}(\overrightarrow{b})\sigma_{inel}^{NN}]^{AB} \end{aligned} \tag{9}$$

The total number of nucleon-nucleon collisions as a function of the scalar impact parameter[1] is

$$N_{coll}(b) = \sum_{n=1}^{AB} nP(n, b) = AB\hat{T}_{AB}(b)\sigma_{inel}^{NN} \tag{10}$$

Now the number of nucleons in the target and projectile nuclei that interact is known as either the number of participants or the number of wounded nucleons. The number of participants as a function of impact parameter $\overrightarrow{b}$, is then given by

$$\begin{aligned} N_{part}(\overrightarrow{b}) = A \int \hat{T}_A(\overrightarrow{s})\{1 - [1 - \hat{T}_B(\overrightarrow{s} - \overrightarrow{b})\sigma_{inel}^{NN}]^B\}d^2s \\ + B \int \hat{T}_B(\overrightarrow{s} - \overrightarrow{b})\{1 - [1 - \hat{T}_A(\overrightarrow{s})\sigma_{inel}^{NN}]^A\}d^2s \end{aligned} \tag{11}$$

where the integral over the bracketed terms gives the respective inelastic cross sections for nucleon-nucleon collisions. The number of participants can also be approximated to equation (12), given that $\sigma_{inel}^{NN}\hat{T}_A(\overrightarrow{b})/A \ll 1$

$$\begin{aligned} N_{part}(\overrightarrow{b}) = \int \hat{T}_A(\overrightarrow{s})\{1 - exp[-\hat{T}_B(\overrightarrow{s} - \overrightarrow{b})\sigma_{inel}^{NN}]\}d^2s \\ + \int \hat{T}_B(\overrightarrow{s} - \overrightarrow{b})\{1 - exp[-\hat{T}_A(\overrightarrow{s})\sigma_{inel}^{NN}]\}d^2s \end{aligned} \tag{12}$$

3.2 Results

In the equations discussed above, only N_{part} and N_{coll} as a function of the impact parameter, b, are illustrated (Fig.(3)), in which the calculations are shown for both the hard sphere model, and also for the Wood-Saxon nucleon distribution model. All calculations were done analytically, and where necessary using numerical integration with the most suitable method for high accuracy. The inelastic nucleon-nucleon cross section was set to 31.5 mb, which averages the cross-section for inelastic interaction within the center of mass energy range of 7 to 60 GeV. Smaller impact parameter in a geometrical picture implies larger overlap, usually termed as central collisions and larger impact parameter collisions have smaller overlap region and termed as peripheral collisions. Hence, N_{part} and N_{coll} decrease with increase in the impact parameter values (Fig.(3)).

4 Relating Glauber Model to experiments

Since neither the value of N_{part} nor the value for N_{coll} can be measured directly in an experiment, we employed

[1] Assuming that the nuclei are not polarized, otherwise one cannot replace the vector impact parameter by a scalar distance.

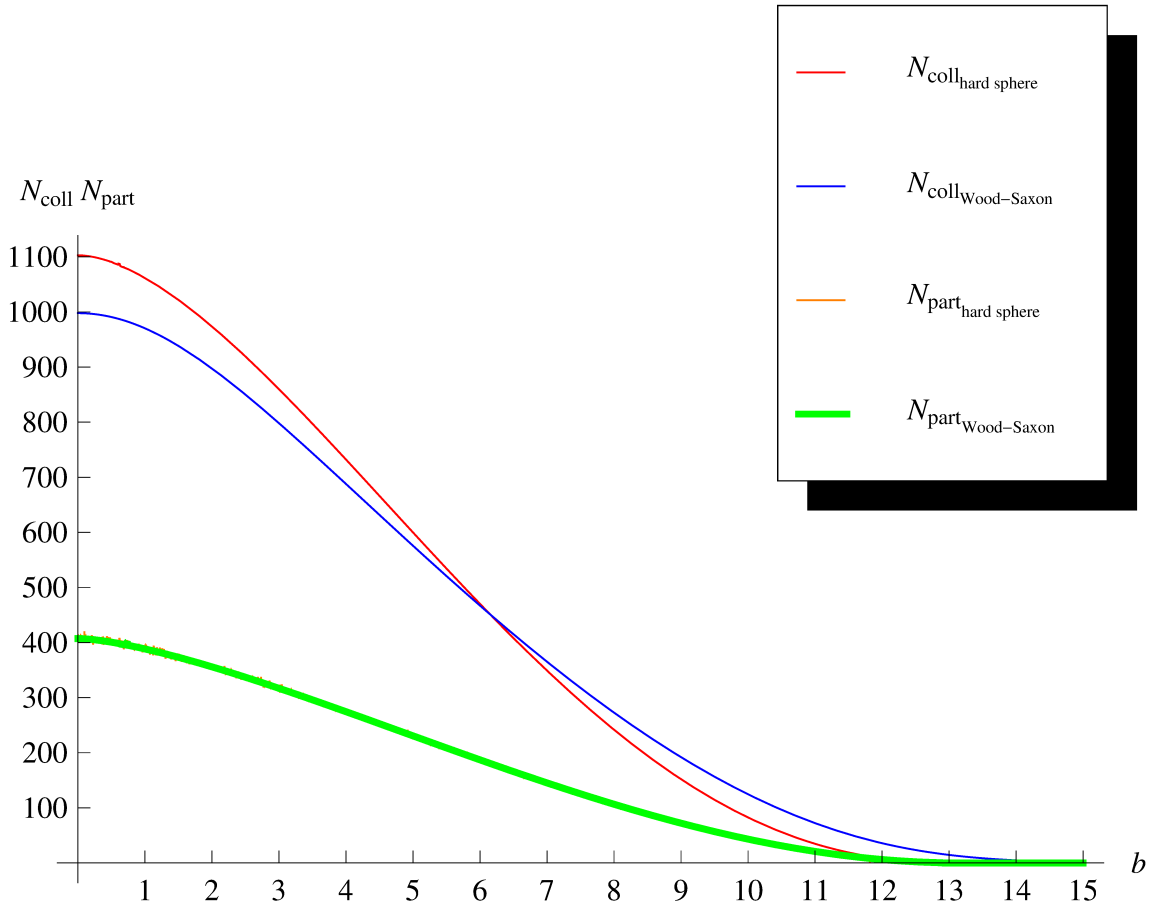

Figure 3: N_{Part} and N_{Coll} as a function of the impact parameter, showing both the hard sphere and the Wood-Saxon model.

a mapping to the number of particles produced in a collision in order to understand the applicability of the Glauber model to experiments. This was done by assuming that a finite amount of particles are being produced in a collision, and a coupling factor was introduced for each particle produced. Indeed, these coupling constants are the measured quantities during an experiment. Then, after assuming that these produced particles follow a Poisson distribution, one could map back to the number of participants in the experiment, with which one can also get the impact parameter by using the Optical Glauber model discussed in the previous section.

4.1 Modeling the production of particles after collision

As already mentioned, a mapping from the produced particles back to the number of participants and then to the impact parameter was implemented. In the following calculations, only two distinct particles are considered, since we are only interested in how the number of produced particles correlate with each other. To a first approximation, it was first assumed that the produced particles follow a Poisson distribution, but as the mean number of particles produced is high, statistically, the Poisson distribution, in the limit of large value of the mean, approximates a Gaussian distribution. So, to a second approximation, the produced particles are assumed to follow a Gaussian distribution, instead of a Poisson, but leaving the variance and the mean equal to each other, as is in the case of a Poisson distribution.

We denote the average number of produced particles by $< N_1 >$ and $< N_2 >$, and define their relation with the number of participants by the following equations,

$$< N_1 >= n_1 N_{part} \tag{13}$$

$$< N_2 >= n_2 N_{part} \tag{14}$$

where n_1 and n_2 are the coupling constants which are measured experimentally. For the purpose of the following calculations, these are set to 10 and 2 respectively, with the values being constrained to experimental results. Also, since the produced particles, N_1 and N_2, follow a Gaussian distribution with mean having the same value as the variance, their probability distribu-

tion functions can be written as follows

$$P_{N_1} = \frac{1}{\sqrt{2\pi < N_1 >}} \exp\left(-\frac{(N_1 - < N_1 >)^2}{2 < N_1 >}\right) \quad (15)$$

$$P_{N_2} = \frac{1}{\sqrt{2\pi < N_2 >}} \exp\left(-\frac{(N_2 - < N_2 >)^2}{2 < N_2 >}\right) \quad (16)$$

In order to get the correlation between these two particles in a range of values of the impact parameter, a two dimensional distribution constituting of the product of the two Gaussian distribution functions for N_1 and N_2 was then considered. This is given by the equation that follows

$$P_{N_1,N_2} = \exp\left(-\frac{(N_1 - < N_1 >)^2}{2 < N_1 >} - \frac{(N_2 - < N_2 >)^2}{2 < N_2 >}\right) \quad (17)$$

Different values of the number of participants where taken from the Optical Glauber model, which then resulted in a range of values for the produced particles, N_1 and N_2,for which a contour plot was then plotted (Fig.(4)). Each contour represents a confidence interval of 1σ with a given impact parameter (Fig.(4)). In fact, it can trivially be shown from equation (17), that these contours are ellipses, and the region for all possible values of N_1 and N_2 with a confidence interval of 1σ was enclosed by the two curves touching the circumference of all produced contours. As the range of the impact parameter is taken infinitesimally small, the whole region will be filled with elliptical contours, and hence a random sample of points (Fig.(4)) was then taken inside this region in order to get a plot on how the correlation between these two produced particles is changing.

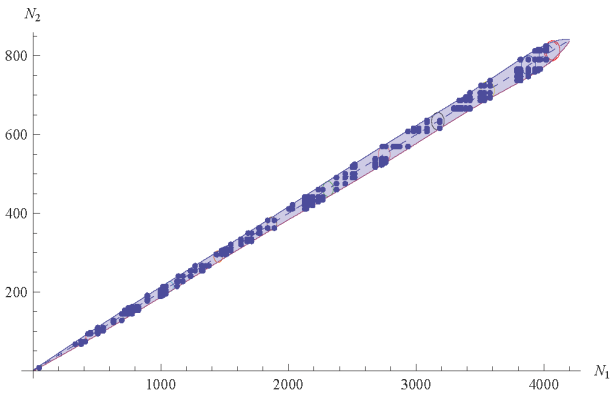

Figure 4: Scatter plot showing the production of two distinct particles, N_1 and N_2.

The correlation between the two produced particles as a function of the impact parameter, is illustrated, in which the dashed line is the analytical fit, whereas the solid line represents the actual points taken from the sample in the defined region (Fig.(5)).

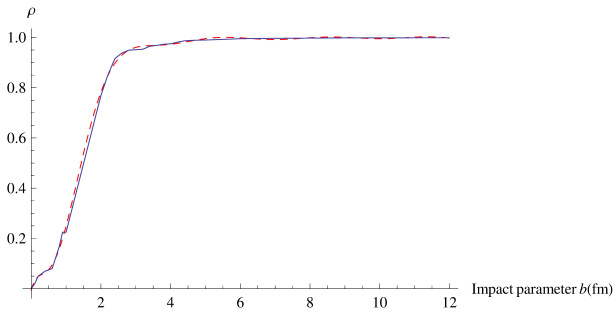

Figure 5: Plot showing the correlation coefficient, ρ, between the produced particles N_1 and N_2 as a function of the impact parameter.

5 Conclusion

The Glauber model as used in ultrarelativistic heavy ion physics is based purely on nuclear geometry. It treats the nucleus-nucleus collision as a series of nucleon-nucleon collision processes. The assumption that A+B collisions can be viewed as a sequence of nucleon-nucleon collisions and that individual nucleons travel on straight-line trajectories comes from its origin as a quantum-mechanical multiple-scattering theory. The Glauber model provides us with the number of participating nucleons and the number of binary collisions for a given impact parameter at a given center of mass energy. With the number of participants, N_{part}, and the number of binary nucleon-nucleon collisions, N_{coll}, the Glauber model introduces quantities that are essentially not measurable. Only the forward energy in fixed-target experiments has a rather direct relation to N_{part}.

One main reason for using geometry-related quantities such as N_{part} calculated with the Glauber model is the possibility of comparing centrality-dependent observables measured in different experiments. Basically all experiments calculate N_{part} and N_{coll} in a similar way using Monte Carlo implementation of the Glauber model so that the theoretical bias introduced in the comparisons is typically small. Thus, the Glauber model provides crucial interface between theory and experiment.

The Glauber model comes in two variants, namely the Optical Glauber model and the Monte Carlo Glauber model. While in the Optical Glauber model the nucleus is considered as a smooth matter density, in the Monte Carlo Glauber model, the nucleons are populated stochastically according to the given nuclear density profile. For the Optical Glauber model, the whole procedure is done analytically, whereas in the Monte Carlo version, it is counted. In the case of this study, only the Optical Glauber approach was considered.

The fact that many ultrarelativistic A+B collisions can be understood purely based on geometry led to a widespread use of the Glauber model. A good example is the total charged-particle multiplicity that scales as

N_{part} over a wide centrality and center-of-mass energy range. Another example is the anisotropic momentum distribution of low-p_T (p_T < 2 GeV/c) particles with respect to the reaction plane. Another important application is in the study of hard scattering processes.

One may conclude that for central collisions, the particles produced are not related with each other, but as soon as the collisions happen to be shifted from the central position, the particles produced will be highly correlated with each other (Fig.(5)). In fact the plot for the correlation as a function of the impact parameter shows that the value of the correlation reaches asymptotically unity very fast, hence showing a very strong correlation between the produced particles (Fig.(5)).

6 Acknowledgements

J.M. gratefully acknowledges the financial support of the CERN Summer Student Programme, during his stay at CERN facilities.

References

Alver B., Baker M., Loizides C. and Steinberg P. (2008) The PHOBOS Glauber Monte Carlo. arXiv:0805.4411v1 [nucl-ex]

Esha R. (2012) Glauber Modeling of High Energy Heavy Ion Collision. Unpublished master's thesis, National Institute of Science Education and Research, Bhubaneswar, India

Miller M.L., Reygers K., Sanders S.J. and Steinberg P. (2007) Glauber Modeling in High-Energy Nuclear Collisions. *Annu. Rev. Nucl. Part. Sci.* 57:205-243.

Appendix 1

Referring to section 4, the particles produced after a collision were assumed to follow a Poisson distribution. One can hence consider a finite amount of produced particles by considering a finite amount of Poisson distributions, not necessarily distinct. Different Poisson distributions, with distinct mean and hence variance, are considered as the produced particles, and the distribution on the right hand side of the plot is the sum of all of these distributions (Fig.(6)). Hence this latter distribution represents the distribution produced by the total amount of particles produced after a collision. We now show that the sum of these Poisson distributions is again a Poisson distribution. We prove further that, since we considered these distributions as Gaussian rather than Poisson, the sum of finite Gaussian distributions is again a Gaussian distribution. Moreover, it can trivially be proved, that the convolution of distinct Gaussian distributions represents actually the sum of Gaussian distributions.

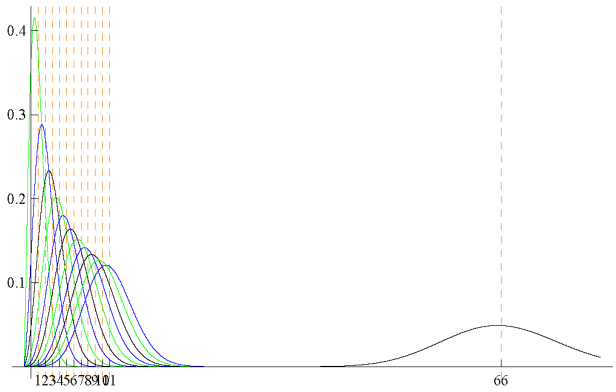

Figure 6: Plot showing a finite number of distinct Poisson distributions on the left hand side, with the sum of these distributions plotted on the right hand side of the plot. The dashed lines represent the mean, and hence the variance of each respective distribution.

We shall prove this result by mathematical induction, although other methods might exist.

We first consider two random variables, N_1 and N_2, to be independent Poisson random variables with parameters $< N_1 >$ and $< N_2 >$. We show that the random variable $N = N_1 + N_2$ is also a Poisson random variable. Indeed, we consider the moment-generating functions, $M_{N_1}(t)$ and $M_{N_2}(t)$, rather than the probability distribution functions of random variables N_1 and N_2, and we use the following theorem in order to prove our result.

Theorem

Let W_1, W_2,..., W_n be independent random variables with moment-generating functions $M_{W_1}(t)$, $M_{W_2}(t)$,..., $M_{W_n}(t)$. Then for the random variable $W = W_1 + W_2 + ... + W_n$, the moment-generating function is given by

$$M_W(t) = M_{W_1}(t) * M_{W_2}(t) * ... * M_{W_n}(t) \qquad (18)$$

Now for a Poisson distribution

$$P_\lambda(k) = \frac{\exp(-\lambda)\lambda^k}{k!} \quad k = 0, 1, 2, ... \qquad (19)$$

the moment-generating function is given by

$$M_\lambda(t) = \exp(-\lambda + \lambda \exp(t)) \qquad (20)$$

Hence,

$$M_{N_1}(t) = \exp(- < N_1 > + < N_1 > \exp(t)) \qquad (21)$$

$$M_{N_2}(t) = \exp(- < N_2 > + < N_2 > \exp(t)) \qquad (22)$$

Hence for the random variable $N = N_1 + N_2$, the theorem implies that

$$\begin{aligned} M_N(t) &= M_{N_1}(t) * M_{N_2}(t) \\ &= \exp(-(< N_1 > + < N_2 >) \\ &+ (< N_1 > + < N_2 >) \exp(t)) \end{aligned} \qquad (23)$$

But this is the moment-generating function of Poisson random variable N, with its parameter being the sum of $< N_1 >$ and $< N_2 >$. Hence, N is a Poisson random variable, being the sum of two independent Poisson random variables.

We now suppose that $N_1, N_2, ..., N_j$ are independent Poisson random variables with parameters $< N_1 >, < N_2 >, ..., < N_j >$ respectively, and that the random variable $N_N = \sum_{k=1}^{j} N_k$ is also a Poisson random variable.

We now show that for $N_1, N_2, ..., N_j, N_{j+1}$ Poisson random variables with parameters $< N_1 >, < N_2 >, ..., < N_j >, < N_{j+1} >$ respectively, the random variable $N_{N+1} = \sum_{k=1}^{j+1} N_k$ is also a Poisson random variable.

Indeed,

$$N_{N+1} = \sum_{k=1}^{j+1} N_k = \sum_{k=1}^{j} N_k + N_{j+1} \tag{24}$$

is a sum of two independent Poisson distributions, which we have already proved that it is again a Poisson distribution. Hence by mathematical induction, we showed that a finite sum of independent Poisson distributions, is again a Poisson distribution.

In a similar way, one can prove by the same argument, that a finite sum of Gaussian distributions, is again a Gaussian distribution. One has to keep in mind that the moment-generating function for a Gaussian distribution is now given by,

$$M_N(t) = \exp\left(\mu t + \frac{1}{2}\sigma^2 t^2\right) \tag{25}$$

where μ and σ are the mean and standard deviation respectively. Moreover, one can also prove that the convolution of Gaussian distributions is the sum of the distributions.